CrystEngComm

PAPER

View Article Online
View Journal | View Issue

Cite this: *CrystEngComm*, 2025, **27**, 5421

Impact of ligand functionalization on the structure of strontium MOFs prepared in a deep eutectic solvent†

Michaël Teixeira and Stéphane A. Baudron *

The 1 : 2 choline chloride : 2-imidazolidinone (e-urea) deep eutectic solvent (DES) was employed for the ionothermal synthesis of strontium-based metal–organic frameworks (Sr-MOFs) using eight dicarboxylic acid-based ligands with varying relative orientations of the two coordinating moieties. With the four linear ligands based on the 2,5-difunctionalized terephthalic acid backbone, the nature of the atom/group at these sites (hydrogen, bromine, trifluoromethyl or hydroxyl) was shown to impact the nature of the secondary building unit (SBU) of the three-dimensional MOFs isolated and characterized by single-crystal X-ray diffraction. Modifying the exocyclic bond angle of the dicarboxylate linker was found to affect both the SBU and dimensionality of the coordination polymer. While the thiophene-based ligand afforded a two-dimensional arrangement, a three-dimensional organization was observed with the furan-based system and a one-dimensional coordination polymer with the isophthalic derivative. Reticulation of the latter system into a three-dimensional MOF was successfully undertaken by the use of the 3,3′,5,5′-azobenzenetetracarboxylic acid ligand comprising two bridged isophthalic acid units, highlighting the robustness of the SBU, in this case. The eight Sr-MOFs obtained feature e-urea molecules bound to the metal cation *via* coordination of the carbonyl unit assisted by hydrogen bonding of the neighbouring NH groups. These coordinated solvent molecules were found to occupy the pores and could unfortunately not be removed *via* thermal activation towards exploitation of the potential porosity. The optical properties of the Sr-MOFs were characterized by absorption and emission spectroscopy. The Sr-MOF based on the 2,5-dihydroxyterephthalic acid ligand was determined to be luminescent (λ_{em} = 575 nm) with a 26% quantum yield in the crystalline state, upon excitation at 360 nm.

Received 14th May 2025,
Accepted 2nd July 2025

DOI: 10.1039/d5ce00497g

rsc.li/crystengcomm

Introduction

Metal–organic frameworks (MOFs) have now been established as an appealing class of crystalline porous materials with applications in various fields such as gas storage and separation, heterogeneous catalysis, energy or drug delivery.[1–5] An important feature of MOFs is their modularity, resulting from their assembly of metal nodes with bridging organic ligands. In particular, the recurrence of secondary building units (SBUs) has been employed as an efficient strategy for the elaboration of new materials.[6] While the coordination chemistry of transition metal cations allows a certain degree of predictability of their SBUs, the situation is not as straightforward with alkaline earth metal ions, for which the coordination numbers and geometry may vary, with a predominance of ionic bonding interactions in the absence of a ligand field stabilization effect.[7–10] This is further complicated by the affinity of these cations towards water, thus acting as a competing ligand. However, investigation of alkaline earth MOFs has been very active, driven by their abundance, low/non-toxicity, and low atomic weight, in particular for Mg(II) and Ca(II). Comparatively, Sr(II)-based MOFs have been generally much less explored.[8]

Recently, we have started studying ionothermal synthesis[11–14] in deep eutectic solvents (DESs)[15–24] as an alternative approach for the preparation of MOFs with a particular emphasis on alkaline earth MOFs.[25–29] These solvents are the combination of two or more compounds showing an important freezing point depression, at the eutectic composition, in comparison with that of their individual components.[15–21] Their wide liquid range, non-flammability, low vapor pressure, their straightforward preparation without the need for purification and their ability to dissolve polar species make them interesting solvents for materials synthesis.[11–24] The vast majority of DESs employed for

Université de Strasbourg, CNRS, CMC UMR 7140, 4 rue Blaise Pascal, F-67000 Strasbourg, France. E-mail: sbaudron@unistra.fr

† Electronic supplementary information (ESI) available: Powder X-ray diffraction patterns, thermogravimetric analyses, and infra-red and diffuse reflectance spectra of Sr-MOFs **1–8**. CCDC 2450477–2450484. For ESI and crystallographic data in CIF or other electronic format see DOI: **https://doi.org/10.1039/d5ce00497g**

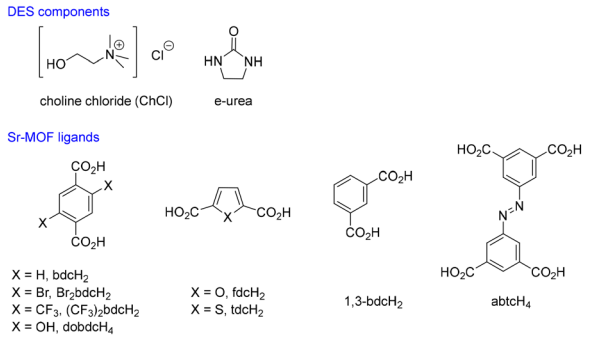

Fig. 1 DES components and ligands explored for the preparation of Sr-MOFs in this work.

the preparation of MOFs are based on the 1 : 2 combination of choline chloride (ChCl, Fig. 1) and urea derivatives. The latter have been shown to impact the crystalline morphology and textural properties of Mg-MOF-74,[27] to allow the formation of an otherwise water-sensitive MOF,[28] and e-urea (2-imidazolidinone, ethylene urea, Fig. 1) was found to lead to a recurrent one-dimensional SBU stabilized by the combination of coordination and hydrogen bonding in Ca-MOFs.[28,29] Interestingly, to the best of our knowledge,[7–14] this type of medium has not been explored for the preparation of Sr-MOFs. We therefore sought to investigate the capacity of the 1 : 2 ChCl : e-urea DES to be used for such purposes with the objective of assessing the ability of this DES to act as an alternative synthetic medium and of evaluating its impact on the resulting Sr-MOFs, with a particular eye on the coordination of the Sr(II) cation and the resulting SBUs, depending on the ligand, as well as on the optical and textural properties of the materials. To this aim, a series of eight Sr-MOFs based on carboxylic acid ligands (Fig. 1) have been prepared and characterized by single-crystal and powder diffraction, thermo-gravimetric and elemental analyses, and infra-red, absorption and emission spectroscopy. The observed SBUs are put in perspective with Ca-MOFs prepared in DESs[28,29] and with reported Sr-MOFs prepared in classical organic solvents and are rationally employed for the elaboration of a three-dimensional network in the case of the isophthalic acid-based system.

Results and discussion

The preparation of Sr-MOFs in the 1 : 2 ChCl : e-urea DES was first explored by heating a mixture of $Sr(NO_3)_2$ with a series of three linear dicarboxylic acids with different functional groups in positions 2 and 5 (terephthalic acid ($bdcH_2$), 2,5-dibromoterephthalic acid (Br_2bdcH_2) and 2,5-bis(trifluoromethyl)terephthalic acid ($(CF_3)_2bdcH_2$) (Fig. 1)) at 120 °C for 2 weeks. Sr-MOF **1**, [Sr(bdc)(e-urea)] crystallizes in the monoclinic $P2_1/n$ space group (Fig. 2 and Table 1). The Sr(II) cation is octacoordinated, bound to four carboxylate units and to the carbonyl moiety of two e-urea molecules, with both types of groups acting as bridges. This leads to the formation of a one-dimensional SBU, along the *b* axis (Fig. 2). The latter is reminiscent of what is observed in

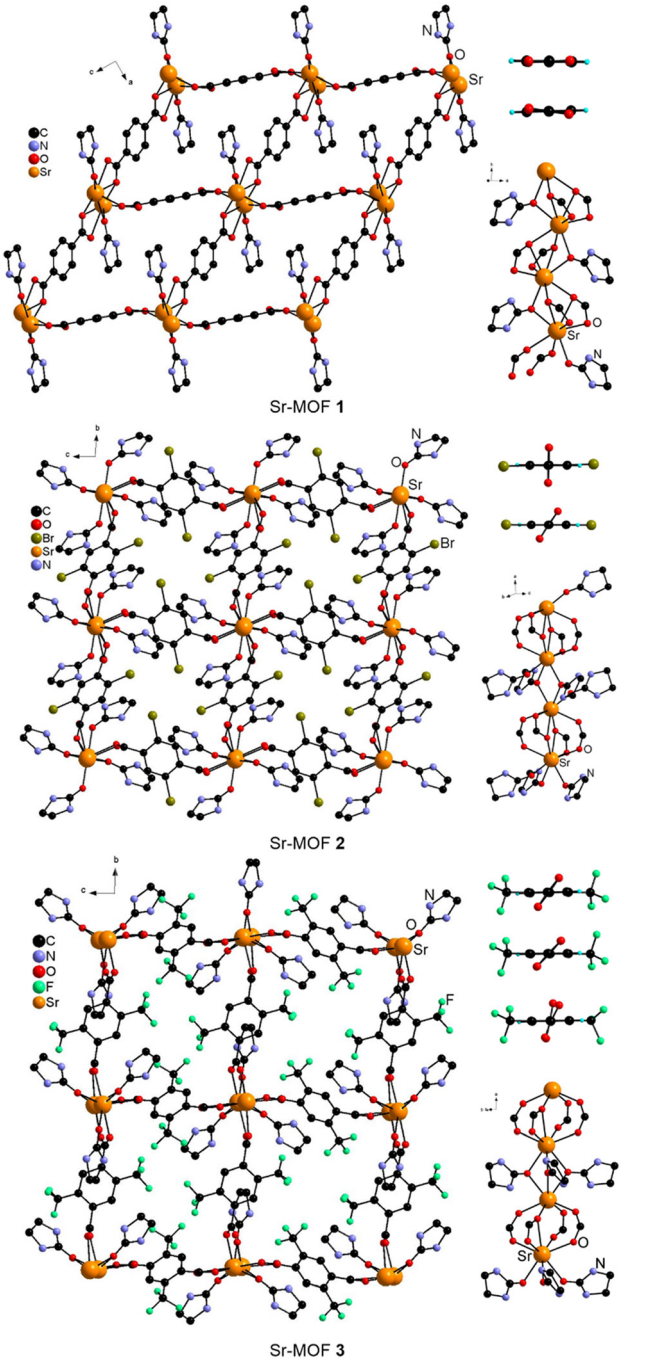

Fig. 2 Views of the crystal structure of Sr-MOFs **1**–**3** and their SBUs. Hydrogen atoms have been omitted and only one position of the disordered CF_3 group in Sr-MOF **3** has been shown, for clarity.

the structure of [Ca(bdc)(e-urea)] and analogues prepared using extended ligands,[28,29] as well as the SBU reported for [Sr(1,4-naphthalene dicarboxylate)(DMF)] (DMF = *N*,*N*-dimethylformamide).[30] Bridging by the terephthalate dianions yields a three-dimensional organization similar to the one described for [Ca(bdc)(e-urea)][28] and [Sr(bdc)(DMF)],[31] where the DMF is terminal. Interestingly, when Br_2bdcH_2 and $(CF_3)_2bdcH_2$ were substituted for $bdcH_2$, [Sr(Br_2bdc)(e-urea)$_2$], Sr-MOF **2**, and [$Sr_2((CF_3)_2bdc)_2$(e-urea)$_3$], Sr-

Table 1 Crystallographic data for Sr-MOFs **1–8**

	1	**2**	**3**	**4**	**5**	**6**	**7**	**8**
Formula	$C_{11}H_{10}N_2O_5Sr$	$C_{14}H_{14}Br_2N_4O_6Sr$	$C_{29}H_{22}F_{12}N_6O_{11}Sr_2$	$C_{11}H_{10}N_2O_7Sr$	$C_{12}H_{14}N_4O_6SSr$	$C_{21}H_{22}N_6O_{13}Sr_2$	$C_{14}H_{16}N_4O_6Sr$	$C_{14}H_{15}N_5O_6Sr$
FW	337.83	581.73	1033.76	369.83	429.95	741.68	423.93	436.93
Crystal system	Monoclinic	Triclinic	Triclinic	Triclinic	Monoclinic	Monoclinic	Tetragonal	Tetragonal
Space group	$P2_1/n$	$P\bar{1}$	$P\bar{1}$	$P\bar{1}$	$C2/c$	$P2_1/n$	$I4_1/a$	$I4_1/a$
a/Å	9.899(2)	8.3624(3)	8.1199(9)	8.5444(14)	30.943(4)	10.7902(3)	22.2525(2)	27.3016(4)
b/Å	7.3502(15)	10.0318(4)	11.4685(12)	8.9657(16)	5.8323(9)	17.9102(4)	22.2525(2)	27.3016(4)
c/Å	17.549(3)	11.0092(4)	20.653(2)	9.8947(18)	17.507(2)	14.8163(4)	13.4124(2)	13.4005(3)
α/°		93.1060(10)	90.290(4)	65.259(5)				
β/°	90.527(7)	90.1830(10)	97.103(4)	87.895(6)	90.591(5)	106.4090(10)		
γ/°		100.0560(10)	90.402(4)	73.816(5)				
V/Å^3	1276.8(5)	907.96(6)	1908.5(3)	658.4(2)	3159.3(8)	2746.69(12)	6641.47(16)	9988.4(4)
Z	4	2	2	2	8	4	16	16
λ/Å	0.71073	0.71073	0.71073	0.71073	0.71073	0.71073	0.67163	1.54178
T/K	120(2)	120(2)	173(2)	173(2)	173(2)	120(2)	100(2)	120(2)
μ mm^{-1}	4.240	7.411	2.918	4.131	3.584	3.960	2.844	3.277
Refls. coll.	31 661	41 117	24 894	20 537	25 289	65 367	58 130	30 058
Ind. refls. (R_{int})	3100 (0.0474)	5321 (0.0471)	9120 (0.1151)	3883 (0.0457)	3798 (0.1127)	7331 (0.0939)	4908 (0.1539)	4403 (0.1751)
R_1 ($I > 2\sigma(I)$)[a]	0.0202	0.0248	0.0494	0.0274	0.0430	0.0357	0.0538	0.0997
wR_2 ($I > 2\sigma(I)$)[a]	0.0427	0.0539	0.0821	0.0542	0.0822	0.0585	0.1076	0.2693
R_1 (all data)[a]	0.0255	0.0340	0.1020	0.0363	0.0789	0.0652	0.0633	0.1232
wR_2 (all data)[a]	0.0450	0.0575	0.0940	0.0569	0.0968	0.0681	0.1123	0.2999
GOF	1.041	1.059	0.864	1.063	1.014	1.046	1.160	1.153

[a] $R_1 = \sum||F_o| - |F_c||/\sum|F_o|$; $wR_2 = [\sum w(F_o^2 - F_c^2)^2/\sum wF_o^4]^{1/2}$.

Table 2 Selected distances within and between the SBUs and geometric parameters (N–H···O distance and angle) of hydrogen bonds involving the e-urea molecule

	$Sr–O_{carboxylate}$/Å	$Sr–O_{e\text{-}urea}$/Å	$Sr–Sr_{withinSBU}$/Å	$Sr–Sr_{betweenSBUs}$/Å	N–H···O/Å	N–H···O/°
1	2.5223(12)–2.6363(12)	2.5476(13)–2.5677(12)	3.8186(7)	10.526(2)	2.812(2)–2.984(2)	147.2–148.8
2	2.5304(15)–2.8073(15)	2.4902(16)–2.6414(16)	4.1786(4)–4.1907(4)	10.0318(5)	2.884(3)–2.998(3)	149.3–161.0
3	2.473(3)–2.951(3)	2.591(3)–2.681(3)	4.0417(7)–4.1522(7)	9.432(1)	2.830(5)–3.122(5)	140.2–155.0
4	2.4529(14)–2.7825(14)	2.4563(15)	4.2351(6)	10.200(2)	2.517(2)	147.1
5	2.488(3)–2.912(3)	2.451(3)	4.1719(7)	8.758(1)	3.024(5)–3.069(4)	147.8–157.9
6	2.449(2)–3.168(2)	2.552(2)–2.622(2)	3.8388(4)–4.1581(4)	9.0665(4)	2.865(3)–3.013(4)	121.1–152.3
7	2.542(2)–2.743(2)	2.570(2)–2.700(2)	3.9829(2)	8.3377(6)	2.811(4)–3.062(4)	132.1–139.0
8	2.545(8)–2.651(8)	2.570(11)–2.740(10)	4.0134(9)	10.931(2)	2.832(6)–3.020(3)	140.3–157.5

MOF **3**, were isolated, both crystallizing in the triclinic $P\bar{1}$ space group (Fig. 2 and Table 1). It can be noted that, to the best of our knowledge, **2** and **3** represent the first examples of Sr-MOFs with these ligands. In **2**, the Sr(II) cation is octacoordinated, bound to four bridging carboxylate units and two bridging and one terminal e-urea molecules. This affords a one-dimensional SBU different from the one observed in **1** with alternating carboxylate groups and e-urea. As a result of the bridging by Br_2bdc^{2-}, a 3D arrangement is observed with channels along the *a* axis, the direction of the SBU (Fig. 2). Similarly, in **3**, the cation is also heptacoordinated but to three bridging e-urea molecules, yielding a 3D organization with channels along the *a* axis.

It is remarkable to note the impact of *ortho* functionalization of the $bdcH_2$ ligand on the Sr-MOF structures. Introduction of either bromo or trifluoromethyl groups at positions 2 and 5 leads to steric hindrance and a modification of the angle between the central phenyl ring and the carboxylate units. While they are almost coplanar in **1** (3.55, 8.06°), they deviate from each other in **2** (55.71, 88.43°) and **3** (46.49, 53.06, 65.36, 78.08°). In all three systems, the coordination of the carbonyl group of the e-urea is supported by hydrogen bonding of the NH moieties with neighbouring carboxylate units with similar bond distances and angles (Table 2). However, the difference in the SBUs is reflected in the longer distances between the Sr(II) cations in **2** and **3** in comparison with **1** (Table 2).

In order to evaluate the impact of additional binding groups on linear dicarboxylic acids, the formation of Sr-MOFs was explored by the reaction of the 2,5-dihydroxyterephthalic acid ligand ($dobdcH_4$) (Fig. 1) with $Sr(NO_3)_2$ in 1 : 2 ChCl : e-urea at 120 °C for 3 weeks. Crystals of **4** formulated as [Sr($dobdcH_2$)(e-urea)] were isolated. Sr-MOF **4** crystallizes in the triclinic $P\bar{1}$ space group and is isostructural to the reported Ca analogue.[28] However, while polymorphism was observed in the case of the Ca-MOF, **4** was isolated as a single crystalline phase as demonstrated by powder X-ray diffraction (Fig. S4†).

This MOF is built around a crystallographically independent Sr(II) cation, two $dobdcH_2^{2-}$ anions on inversion centers and an e-urea molecule. The metal center is heptacoordinated, bound to four carboxylates, two hydroxyl groups and the solvent molecule (Fig. 3). Interestingly, out of the two anions, only one features coordination *via* the hydroxyl moieties, whereas the other is bound solely *via* the carboxylates (Fig. 3c and d). This differs from reported [Sr($dobdcH_2$)(H_2O)], CPO-22,[32] and [Sr_3($dobdcH_2$)$_3$($DMAc$)$_6$](H_2O) (DMAc = *N*,*N*-dimethylacetamide),[33] where a single type of coordination is observed, either involving all the OH groups or none, respectively. The latter functions are coplanar with the central aromatic ring, further stabilized by intramolecular hydrogen bonding with the OH groups (Fig. 3 and Table 2). Bridging by the ligands leads to a 3D arrangement with channels occupied by coordinated e-urea.

In order to explore the influence of the relative position of the coordinating groups, other ligands featuring varying exocyclic bond angles of the dicarboxylate linker, θ, were investigated: 2,5-thiophenedicarboxylic acid ($tdcH_2$, θ = 148°), 2,5-furandicarboxylic acid ($fdcH_2$, θ = 125°) and isophthalic acid (1,3-$bdcH_2$, θ = 120°) (Fig. 1). It has indeed been reported that θ has a great influence on the structure of coordination cages and MOFs.[34–36]

First, 2,5-thiophenedicarboxylic acid, $tdcH_2$ (Fig. 1), was used for the preparation of [Sr(tdc)(e-urea)](e-urea), Sr-MOF **5** (monoclinic, $C2/c$ (Table 1)). In **5**, the Sr(II) cation is in an octahedral coordination environment, bound to five bridging carboxylate moieties and one terminal e-urea molecule

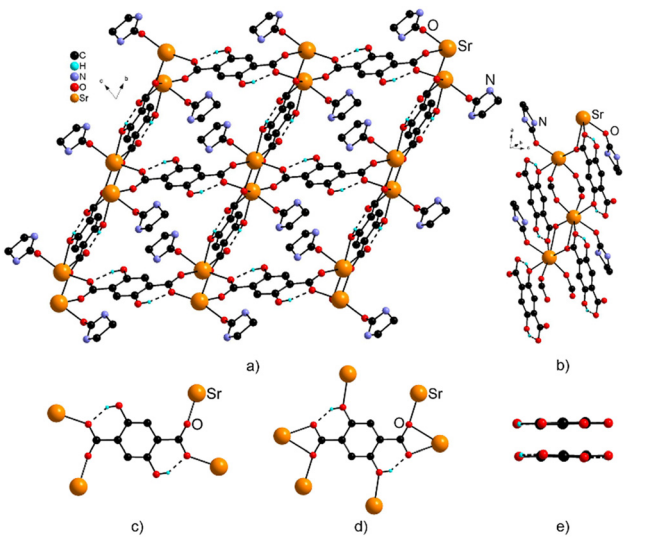

Fig. 3 View along the *a* axis of the structure of Sr-MOF **4** (a), of its SBU (b), and of the two coordination modes of the $dobdcH_2^{2-}$ ligands (c and d) and side view of the ligands (e). CH and NH hydrogen atoms have been omitted for clarity.

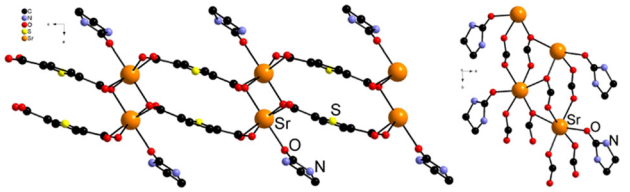

Fig. 4 View of the 2D arrangement in Sr-MOF **5** (left) and of the SBU (right). Hydrogen atoms have been omitted for clarity.

(Fig. 4). This leads to the formation of a 2D-arrangement, with layers separated by an additional e-urea solvate molecule that is hydrogen bonded to the NH group of the coordinated e-urea. It can be noted that Sr-MOF **5** differs from the other reported Sr-MOFs incorporating tdc^{2-}, prepared from DMF or DMAc, featuring a 3D arrangement with Sr cations, and either hepta- or octacoordinated.[37,38]

Modifying the nature of the heteroatom from $tdcH_2$ to $fdcH_2$ (Fig. 1) led to the formation of $[Sr_2(fdc)_2(e\text{-}urea)_3]$, Sr-MOF **6**, crystallizing in the monoclinic $P2_1/n$ space group (Table 1). One of the two crystallographically independent Sr(II) cations is octa-coordinated, bound to two bridging e-urea molecules and four carboxylate moieties, while the other is heptacoordinated, ligated to an additional terminal e-urea molecule (Fig. 5). This leads to a 3D arrangement with channels occupied by coordinated solvent molecules (Fig. 5). It is worth noting that the change in the exocyclic bond angle θ of the dicarboxylate linker has such an impact on the SBU and dimensionality of the Sr-MOF.

Then, the use of isophthalic acid (1,3-$bdcH_2$, Fig. 1) was considered. Heating a mixture of this ligand with $Sr(NO_3)_2$ in the 1 : 2 ChCl : e-urea DES at 120 °C for 4 weeks afforded $[Sr(1,3\text{-}bdc)(e\text{-}urea)_2]$, Sr-MOF **7**, crystallizing in the tetragonal $I4_1/a$ space group (Table 1). The Sr(II) cation is octacoordinated, bound to four bridging carboxylates and two e-urea molecules, one in the terminal position and the other acting as a bridging ligand (Fig. 6). Owing to the structure of the 1,3-bdc^{2-} anion, the metal centers are organized into a 1D SBU, yielding a 1D coordination polymer.

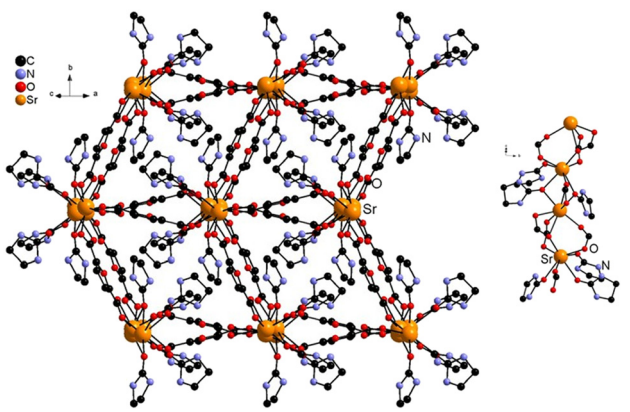

Fig. 5 View of the structure of Sr-MOF **6** (left) and of its SBU (right). Hydrogen atoms have been omitted for clarity.

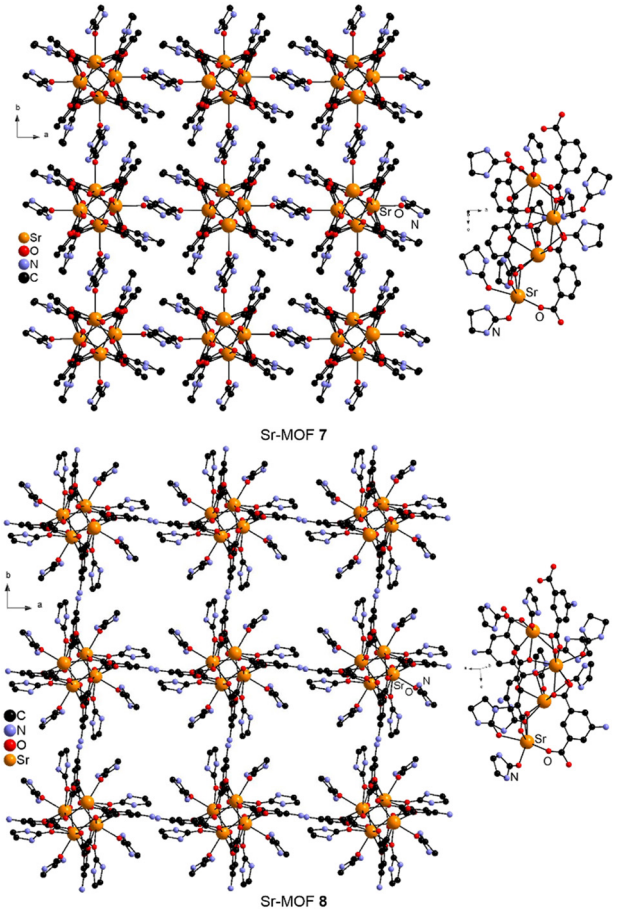

Fig. 6 Views of the crystal structure of Sr-MOFs **7** and **8** and their SBUs. Hydrogen atoms have been omitted and only one position of the disordered e-urea molecule in Sr-MOF **6** has been shown, for clarity.

This arrangement differs from the one reported for $[Sr_2(1,3\text{-}bdc)_2(H_2O)_2](H_2O)$ showing a 2D organization.[39]

It is interesting to note that these 1D chains are arranged in a parallel fashion with the C_5 carbon atom of the 1,3-bdc^{2-} anion of the neighbouring chain at a distance of 5.118(5) Å. Provided that this SBU is a robust motif, one may consider the formation of a 3D arrangement using ligands based on bridged isophthalic acid moieties to connect the 1D chains. The formation of Sr-MOFs based on such bridged ligands has been reported under conventional solvothermal conditions.[40–50] Surprisingly, while the 3,3′,5,5′-azobenzenetetracarboxylic acid ($abtcH_4$, Fig. 1), an interesting target ligand, has been shown to form Mg-MOFs[51,52] and Ca-MOFs,[53,54] the preparation of Sr analogues has not been described. The reaction of $abtcH_4$ with $Sr(NO_3)_2$ in the 1 : 2 ChCl : e-urea DES at 120 °C for 4 weeks afforded $[Sr_2(abtc)(e\text{-}urea)_4]$, Sr-MOF **8**. As **7**, **8** crystallizes in the tetragonal $I4_1/a$ space group (Table 1) and, remarkably, the SBU observed in **7** is maintained in **8** (Fig. 6 and Table 2). Therefore, as anticipated, the structure of the diazo $abtc^{4-}$ ligand with its two connected isophthalate moieties leads to bridging of the SBUs, hence affording a 3D MOF (Fig. 6). This result opens the door to a reticulation approach towards the formation of Sr-MOFs.

The MOFs were characterized by powder X-ray diffraction to assess whether a single phase has formed (Fig. S1–8†). While a good match between the pattern calculated from single-crystal data and the experimental one was observed for **1**–**7**, the patterns differ for **8**. For the latter material, this suggests the presence of different crystalline systems in addition to the one for which single-crystal data could be obtained. It is consistent with our inability so far to obtain acceptable results from elemental analysis of **8**. These results could unfortunately not be rationalized in a reasonable composition. Analysis by infra-red spectroscopy (Fig. S16†) did not show the presence of the remaining ligand, therefore supporting the formation of another MOF, which could not be isolated/identified under the synthetic conditions leading to **8**. For the other systems, **1**–**7**, characterization by infra-red spectroscopy (Fig. S9–15†) also confirmed the absence of starting ligands as demonstrated in particular in the area between 1500 and 1700 cm^{-1} showing the disappearance of the ν(C=O) stretching mode in favour of the $\nu_{as}(COO^{-})$ mode of the carboxylate upon coordination to the Sr(II) cation and formation of the MOFs.[55] The purity of these compounds was further confirmed by elemental analysis. It is worth noting, however, that for **1**, an alternative synthesis under urothermal conditions[56] was employed to obtain the MOF in pure form.

The Sr-MOFs were characterized by thermo-gravimetric analysis to investigate the possibility of removing the e-urea molecules plugging the potential pores (Fig. S17–23†). For **1**–**7**, a weight loss with an onset between 250 and 300 °C accounting for more than the expected weight of the e-urea present in the material was observed. This suggests decomposition of the product before the removal of the solvent molecules, thus hindering further investigation towards thermal activation of these MOFs. A similar behaviour has been observed with Ca-MOFs prepared from the 1 : 2 ChCl : e-urea DES where the solvent molecules allows the formation of a robust SBU but cannot be removed without collapse of the framework.[28,29] Analogous thermal stability is also observed for other Sr-MOFs based on ligands incorporating a 2-hydroxylbenzoic acid motif.[57,58] Although **8** features an interesting structure, its above-mentioned lack of purity prevented us to further characterize it.

Since some Sr-MOFs have been reported to be emissive,[8,33,38,40–50] the absorption and luminescence properties of MOFs **1**–**7** were investigated. The diffuse reflectance spectra of **1**–**3** and **5**–**7** show a broad band with a maximum at around 280–320 nm, whereas this maximum is at around 400 nm for **4** (Fig. S24–30†). Interestingly, only Sr-MOF **4** showed a measurable emission. Upon excitation at 360 nm, luminescence at 575 nm could be observed with a red shift when compared with the emission of the free $dobdcH_4$ ligand (λ_{em} = 470 nm) (Fig. 7). This is consistent with what has been reported for the isostructural Ca analogue, $[Ca(dobdcH_2)(e\text{-urea})]$,[28] and $[Sr_3(dobdcH_2)_3(DMAc)_6](H_2O)$.[33] In the latter reported compound,[33] a thorough investigation of the photophysical properties has demonstrated the co-existence of two different

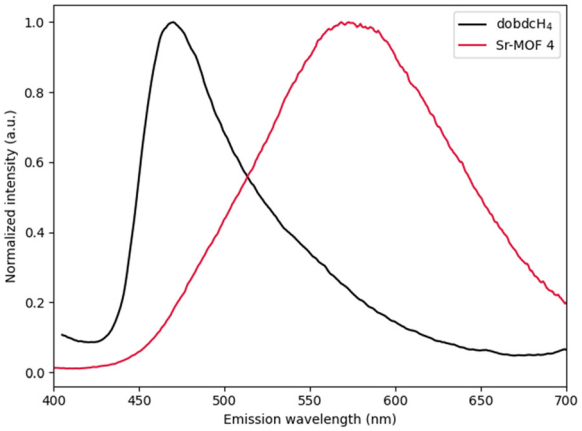

Fig. 7 Solid state emission spectra of ligand $dobdcH_4$ (black) and Sr-MOF **4** (red) upon excitation at 360 nm, at room temperature.

emitting states. The first one results from relaxation of the S_1 excited state, while the other one derives from excited state intramolecular proton transfer (ESIPT).[59] Both states can contribute with varying degrees to the emission depending on the temperature, the nature of the metal center and the coordination mode. In particular, it has been shown theoretically and experimentally that, while the emission derives mostly from the singlet state, coordination to the hydroxyl group of heavier cations, such as Sr(II), favours the contribution of emissive relaxation from the lower lying excited state formed after ESIPT.[33] A quantum yield of 26% was determined for **5**, similar to the ones reported for $[Sr_3(dobdcH_2)_3(DMAc)_6](H_2O)$ and $[Ba(dobdcH_2)(DMAc)]$,[33] showing similar coordination modes of the ligand, and significantly higher than for other Sr-MOFs based on dicarboxylates.[60,61]

Conclusion

The 1 : 2 ChCl : e-urea DES was employed for the ionothermal synthesis of Sr-MOFs using eight dicarboxylic acid-based ligands with varying relative orientations of the two coordinating moieties. For the three linear ligands ($bdcH_2$, Br_2bdcH_2 and 2,5-$(CF_3)_2bdcH_2$), 3D MOFs were obtained with coordinated e-urea plugging the channels. However, the functional groups in positions 2 and 5 were shown to impact the observed SBU, albeit all featuring bridging e-urea. Interestingly, introduction of coordinating hydroxyl groups at these positions with the $dobdcH_4$ ligand led to a MOF with a terminal solvent molecule. This MOF, **4**, was also found to be luminescent in the solid state (ϕ = 26%). To further explore the impact of the ligand structure, a series of derivatives with varying exocyclic bond angles of the dicarboxylate linker were investigated. While the thiophene-based ligand afforded a 2D arrangement, a 3D organization was observed with the furan-based system and a 1D coordination polymer with the 1,3-$bdcH_2$ derivative. The latter system is noteworthy as it features a one-dimensional SBU with terminal e-urea. Reticulation of the latter system into a three-dimensional MOF was successfully undertaken by the use of the $abtcH_4$

ligand comprising two bridged isophthalic acid units, highlighting the robustness of the SBU in this case. However, since this MOF could not be obtained in pure form, this material could unfortunately not be further studied.

The foregoing results have demonstrated the capacity of the 1 : 2 ChCl : e-urea DES to be a medium for the formation of Sr-MOFs. While a parallel can be drawn with solvents such as DMF for such purposes given that its decomposition yields amines allowing deprotonation of the carboxylic acid-based ligand[27] and its coordination to the metal cation leads to a diversity of SBUs, this alternative solvent for the preparation of Sr-MOFs has its downside. As observed for Ca-MOFs prepared under analogous ionothermal conditions, the e-urea molecules are systematically bound to the metal cation and occupy the channels, rendering thermal activation towards accessing the potential porosity of the MOFs impossible. While the presence of NH groups assisting the coordination of the carbonyl unit leads to a robust binding motif, it may also be responsible for the difficulty in activating the materials. This observation along with the absence of ChCl in any of the structures obtained raises the question of exploring the preparation of alkaline earth MOFs under urothermal conditions[56] using a fully alkylated urea derivative. This approach is currently under investigation and will be published in due course.

Experimental

Synthesis

DES preparation. The ChCl : e-urea 1 : 2 DES was freshly prepared before each synthesis by heating a mixture of one equivalent of ChCl and two equivalents of e-urea at 90 °C under agitation in a round-bottom flask, until a homogeneous liquid phase was formed. To avoid solidification of the DES (m.p. = 70 °C), it was transferred to a vial while hot using preheated syringes.

General MOF synthesis procedure. The reagents were added to a vial before addition of the solvent. The vial was then heated in a dry bath. After completion of the reaction and before letting the vial cool down, ethanol was added to prevent solidification. The resulting mixture was then filtered and washed multiple times with ethanol. The remaining solid was air-dried.

Sr-MOF 1 [Sr(bdc)(e-urea)]. Ionothermal method: terephthalic acid (0.033 g, 0.2 mmol) and $Sr(NO_3)_2$ (0.085 g, 0.4 mmol) were added to an 8 mL vial before addition of freshly prepared ChCl : e-urea DES (1 : 2, 2.5 mL). The vial was then heated at 120 °C for 2 weeks. The reaction was treated according to the general procedure. No pure sample could be obtained with this method.

Urothermal method: terephthalic acid (0.033 g, 0.2 mmol) and $Sr(NO_3)_2$ (0.085 g, 0.4 mmol) were added to an 8 mL vial before addition of e-urea hemihydrate (4 g). The vial was then heated at 120 °C for 2 weeks. The reaction was treated according to the general procedure (0.0398 g, 58.9%). Elemental analysis (CHN) for $C_{11}H_{10}N_2O_5Sr$; calculated: C, 39.11; H, 2.98; N, 8.29; found: C, 39.00; H, 2.97; N, 8.36.

Sr-MOF 2 [Sr(Br$_2$bdc)(e-urea)$_2$]. 2,5-Dibromoterephthalic acid (0.032 g, 0.1 mmol) and $Sr(NO_3)_2$ (0.042 g, 0.2 mmol) were added to an 8 mL vial before addition of freshly prepared ChCl : e-urea DES (1 : 2, 2.5 mL). The vial was then heated at 120 °C for 2 weeks. The reaction was treated according to the general procedure (0.0315 g, 54.3%). Elemental analysis (CHN) for $C_{14}H_{14}Br_2N_4O_6Sr$; calculated: C, 28.91; H, 2.43; N, 9.63; found: C, 28.99; H, 2.50; N, 9.71.

Sr-MOF 3 [Sr$_2$((CF$_3$)$_2$bdc)$_2$(e-urea)$_3$]. 2,5-Bis(trifluoromethyl) terephthalic acid (0.015 g, 0.05 mmol) and $Sr(NO_3)_2$ (0.021 g, 0.1 mmol) were added to an 8 mL vial before addition of freshly prepared ChCl : e-urea DES (1 : 2, 2.5 mL). The vial was then heated at 120 °C for 2 weeks. The reaction was treated according to the general procedure (0.0098 g, 37.9%). Elemental analysis (CHN) for $C_{29}H_{22}F_{12}N_6O_{11}Sr_2$; calculated: C, 33.69; H, 2.15; N, 8.13; found: C, 33.78; H, 2.30; N, 8.69.

Sr-MOF 4 [Sr(dobdcH$_2$)(e-urea)]. 2,5-Dihydroxyterephthalic acid (0.020 g, 0.1 mmol) and $Sr(NO_3)_2$ (0.042 g, 0.2 mmol) were added to an 8 mL vial before addition of freshly prepared ChCl : e-urea DES (1 : 2, 2.5 mL). The vial was then heated at 120 °C for 3 weeks. The reaction was treated according to the general procedure (0.0044 g, 11.9%). Elemental analysis (CHN) for $C_{11}H_{10}N_2O_7Sr$; calculated: C, 35.72; H, 2.73; N, 7.57; found: C, 35.49; H, 2.83; N, 7.89.

Sr-MOF 5 [Sr(tdc)(e-urea)](e-urea). 2,5-Thiophenedicarboxylic acid (0.034 g, 0.2 mmol) and $Sr(NO_3)_2$ (0.085 g, 0.4 mmol) were added to an 8 mL vial before addition of freshly prepared ChCl : e-urea DES (1 : 2, 2.5 mL). The vial was then heated at 120 °C for 3 weeks. The reaction was treated according to the general procedure (0.0537 g, 62.0%). Elemental analysis (CHN) for $C_{12}H_{14}N_4O_6SSr$; calculated: C, 33.52; H, 3.28; N, 13.03; found: C, 32.96; H, 3.16; N, 12.20.

Sr-MOF 6 [Sr$_2$(fdc)$_2$(e-urea)$_3$]. 2,5-Furandicarboxylic acid (0.062 g, 0.2 mmol) and $Sr(NO_3)_2$ (0.085 g, 0.4 mmol) were added to an 8 mL vial before addition of freshly prepared ChCl : e-urea DES (1 : 2, 2.5 mL). The vial was then heated at 120 °C for 2 weeks. The reaction was treated according to the general procedure (0.0530 g, 71.5%). Elemental analysis (CHN) for $C_{21}H_{22}N_6O_{13}Sr_2$; calculated: C, 34.01; H, 2.99; N, 11.33; found: C, 33.88; H, 2.99; N, 11.28.

Sr-MOF 7 [Sr(1,3-bdc)(e-urea)$_2$]. Isophthalic acid (0.033 g, 0.2 mmol) and $Sr(NO_3)_2$ (0.042 g, 0.2 mmol) were added to an 8 mL vial before addition of freshly prepared ChCl : e-urea DES (1 : 2, 2.5 mL). The vial was then heated at 120 °C for 4 weeks. The reaction was treated according to the general procedure (0.0582 g, 68.4%). Elemental analysis (CHN) for $C_{14}H_{16}N_4O_6Sr$; calculated: C, 39.67; H, 3.80; N, 13.22; found: C, 38.40; H, 3.88; N, 12.21.

Sr-MOF 8 [Sr$_2$(abtc)(e-urea)$_4$]. 3,3′,5,5′-Azobenzene tetracarboxylic acid (0.018 g, 0.05 mmol) and $Sr(NO_3)_2$ (0.042 g, 0.2 mmol) were added to a 20 mL vial before addition of freshly prepared ChCl : e-urea DES (1 : 2, 10 mL). The vial was then heated at 120 °C for 4 weeks. The reaction was treated according to the general procedure. Elemental analysis (CHN) for $C_{28}H_{30}N_{10}O_{12}Sr_2$; calculated: C, 38.49; H, 3.46; N, 16.03; found: C, 34.30; H, 4.43; N, 13.47. To the best of our

ability, we were not able to obtain a pure sample of the compound, as demonstrated by elemental analysis and X-ray power diffraction (Fig. S8†).

X-ray diffraction

X-Ray diffraction data collection for **1**, **2**, **6** and **8** was carried out on a Bruker PHOTON-III DUO CPAD diffractometer equipped with an Oxford Cryosystem liquid N_2 device, using Mo-Kα radiation (λ = 0.71073 Å) at 120 K. X-ray diffraction data collection for **3**, **4** and **5** was carried out on a Bruker APEX II DUO Kappa-CCD diffractometer equipped with an Oxford Cryosystem liquid N_2 device, using Mo-Kα radiation (λ = 0.71073 Å) at 173 K. The structures were solved using the program SHELXT-2018.[62] The refinement and all further calculations were carried out using SHELXL-2018.[63] The H-atoms were included in calculated positions and treated as riding atoms using SHELXL default parameters. The non-H atoms were refined anisotropically, using weighted full-matrix least-squares on F^2. A semi-empirical absorption correction was applied using SADABS in APEX4.[64]

The single-crystal X-ray diffraction data acquisition of **7** was carried out at the CRISTAL beamline (synchrotron SOLEIL, Paris) using the synchrotron radiation source (λ = 0.67199 Å). Diffracted intensities were measured using a CCD detector (Atlas detector from Rigaku) mounted on a four-circle MKS-Newport diffractometer. The crystal-to-detector distance was set to 80 mm. The temperature of the data collection (T = 100 K) was reached with a gas streamer (CryoIndustries of America). The wavelength was selected with a double crystal monochromator (Si 111 crystals) and sagittal (horizontal) focusing was achieved using a 1D SU-8 compound refractive lens system developed by the Karlsruhe Institute of Technology. The beam attenuation was performed using Al (or Cu) foil of different thicknesses inserted in the incident beam. Data collection strategies, refinement of the unit cell parameters and data reduction were carried out using the CrysAlisPro software package.[65] The refinement and all further calculations were carried out using SHELXL-2018.[63]

Powder X-ray diffraction patterns were recorded at 293 K on a Bruker D8 diffractometer using monochromatic Cu-Kα radiation with a scanning range between 3 and 40° using a scan step of 1.17° min^{-1}, with the compound placed on a rotating Si low background sample holder. The calculated diagrams were generated with the Mercury® software based on the single-crystal data collected.

Thermo-gravimetric analysis

The thermal stability of the samples was determined on a PerkinElmer thermogravimetric analyzer TGA 4000 under a N_2 flow of 20 mL min^{-1} and at a heating rate of 5 °C min^{-1} up to 800 °C.

Optical properties

Diffuse reflectance spectra were collected on a PerkinElmer Lambda 650S UV-vis spectrometer at room temperature. Emission spectra were collected on a PerkinElmer LS55 fluorescence spectrometer at room temperature.

Quantum yield was determined on a Hamamatsu Quantaurus QY absolute PL quantum yield spectrometer C11347.

Infra-red spectroscopy

Infra-red spectra were collected at room temperature on a Perkin-Elmer FTIR-UATR Spectrum Two spectrometer by attenuated total reflectance on powders.

Elemental analysis

Elemental analyses (CHN) were performed at the Service Commun d'Analyses of the University of Strasbourg, in duplicate, employing ThermoFisher FLASH 2000 equipment, whereas the reported values for CHN were taken as the average of two measurements.

Data availability

The data supporting this article (powder X-ray diffraction patterns, thermogravimetric analyses, and infra-red and diffuse reflectance spectra of Sr-MOFs **1**–**8**) have been included as part of the ESI.† Crystallographic data for Sr-MOFs **1**–**8** have been deposited at the CCDC under 2450477–2450484.

Author contributions

Investigation: M. T. and S. A. B.; methodology: M. T. and S. A. B.; writing – original draft: S. A. B.; writing – review & editing: M. T. and S. A. B.; funding acquisition: S. A. B.

Conflicts of interest

There are no conflicts to declare.

Acknowledgements

We thank the Université de Strasbourg, the C.N.R.S., and the Ministère de l'Enseignement Supérieur, de la Recherche et de l'Innovation (Ph. D. fellowship of Michaël Teixeira) for financial support. This work was supported by the Interdisciplinary Thematic Institute SysChem, *via* the IdEx Unistra (ANR-10-IDEX-0002) and by the CSC Graduate School (CSC-IGS ANR-17-EURE-0016) within the French Investments for the Future Program. We thank Corinne Bailly and Nathalie Gruber (Service de radiocristallographie de la Fédération de Chimie Le Bel – UAR 2042) for assistance in the crystal structure determination of **1**, **2**, **6** and **8**. We acknowledge SOLEIL for provision of synchrotron radiation facilities and we would like to thank Dr. Pierre Fertey for assistance in using beamline CRISTAL (BAG 20221035) and we also thank Dr. Jaison Casas and Prof. Véronique Bulach (University of Strasbourg) for assistance in the diffraction data collection of **7**. We thank Dr. Guillaume Rogez and Ludovic Lepee (IPCMS, Strasbourg) for their help in determining the solid-state quantum yields.

References

1 H. C. Zhou, J. R. Long and O. M. Yaghi, *Chem. Rev.*, 2012, **112**, 673, Metal-organic frameworks special issue.
2 H. C. J. Zhou and S. Kitagawa, *Chem. Soc. Rev.*, 2014, **43**, 5415, themed issue on metal-organic frameworks.
3 M. Dincă and J. R. Long, *Chem. Rev.*, 2020, **120**, 8037, Porous framework chemistry special issue.
4 E. Linnane, S. Haddad, F. Melle, Z. Mei and D. Fairen-Jimenez, *Chem. Soc. Rev.*, 2022, **51**, 6065.
5 A. Iliescu, J. J. Oppenheim, C. Sun and M. Dincă, *Chem. Rev.*, 2023, **123**, 6197.
6 D. J. Tranchemontagne, J. L. Mendoza-Cortés, M. O'Keeffe and O. M. Yaghi, *Chem. Soc. Rev.*, 2009, **38**, 1257.
7 D. Banerjee and J. B. Parise, *Cryst. Growth Des.*, 2011, **11**, 4704.
8 Y. Zang, L.-K. Li and S.-Q. Zang, *Coord. Chem. Rev.*, 2021, **440**, 213955.
9 M. A. Alnaqbi, A. Alzamly, S. Hussein Ahmed, M. Bakiro, J. Kegere and H. L. Nguyen, *J. Mater. Chem. A*, 2021, **9**, 3828.
10 S. Xian, Y. Lin, H. Wang and J. Li, *Small*, 2021, **17**, 2005165.
11 R. E. Morris, *Chem. Commun.*, 2009, 2990.
12 B. Zhang, J. Zhang and B. Han, *Chem. – Asian J.*, 2016, **11**, 2610.
13 P. Li, F.-F. Cheng, W.-W. Xiong and Q. Zhang, *Inorg. Chem. Front.*, 2018, **5**, 2693.
14 R. A. Maia, B. Louis and S. A. Baudron, *CrystEngComm*, 2021, **23**, 5016.
15 Q. Zhang, K. de Oliveira Vigier, S. Royer and F. Jérôme, *Chem. Soc. Rev.*, 2012, **41**, 7108.
16 E. L. Smith, A. P. Abbott and K. S. Ryder, *Chem. Rev.*, 2014, **114**, 11060–11082.
17 B. Gurkan, H. Squire and E. Pentzer, *J. Phys. Chem. Lett.*, 2019, **10**, 7956–7964.
18 B. B. Hansen, S. Spittle, B. Chen, D. Poe, Y. Zhang, J. M. Klein, A. Horton, L. Adhikari, T. Zelovich, B. W. Doherty, B. Gurkan, E. J. Maginn, A. Ragauskas, M. Dadmun, T. A. Zawodzinski, G. A. Baker, M. E. Tuckerman, R. F. Savinell and J. R. Sangoro, *Chem. Rev.*, 2021, **121**, 1232.
19 D. Yu, Z. Xue and T. Mu, *Chem. Soc. Rev.*, 2021, **50**, 8596.
20 M. A. R. Martins, S. P. Pinho and J. A. P. Coutinho, *J. Solution Chem.*, 2019, **48**, 962.
21 D. O. Abranches and J. A. P. Coutinho, *Annu. Rev. Chem. Biomol. Eng.*, 2023, **14**, 141.
22 J. Hu, J. Zhang, Y. Zhao and Y. Yang, *Chem. Commun.*, 2024, **60**, 2887.
23 B. Mahto, H. Ali, A. Barhoi and S. Hussain, *Coord. Chem. Rev.*, 2025, **527**, 216406.
24 Z. Wang, X. Zhao, Y. Chen, C. Wei and J. Jiang, *RSC Sustainability*, 2025, **3**, 738.
25 R. A. Maia, B. Louis and S. A. Baudron, *Dalton Trans.*, 2021, **50**, 4145.
26 R. A. Maia, A. Fluck, C. Maxim, B. Louis and S. A. Baudron, *Green Chem.*, 2023, **25**, 9103.
27 M. Teixeira, R. A. Maia, S. Shanmugam, B. Louis and S. A. Baudron, *Microporous Mesoporous Mater.*, 2022, **343**, 112148.
28 M. Teixeira, R. A. Maia, L. Karmazin, B. Louis and S. A. Baudron, *CrystEngComm*, 2022, **24**, 601.
29 M. Teixeira, B. Louis and S. A. Baudron, *Dalton Trans.*, 2025, **54**, 5006.
30 C. A. Williams, A. J. Blake, P. Hubberstey and M. Schröder, *Cryst. Growth Des.*, 2008, **8**, 911.
31 D. Guo, C.-M. Liang, K. Chiu and W.-K. Wang, *Z. Anorg. Allg. Chem.*, 2021, **647**, 1193.
32 P. D. C. Dietzel, R. Blom and H. Fjellvåg, *Z. Anorg. Allg. Chem.*, 1953, **2009**, 635.
33 A. Douvali, G. S. Papaefstathiou, M. P. Gullo, A. Barbieri, A. C. Tsipis, C. D. Malliakas, M. G. Kanatzidis, I. Papadas, G. S. Armatas, A. G. Hatzidimitriou, T. Lazarides and M. J. Manos, *Inorg. Chem.*, 2015, **54**, 5813.
34 K. Harris, D. Fujita and M. Fujita, *Chem. Commun.*, 2013, **49**, 6703.
35 J. Yang, M. Lutz, A. Grzech, F. M. Mulder and T. J. Dingemans, *CrystEngComm*, 2014, **16**, 5121.
36 C. Hua and D. M. D'Alessandro, *Cryst. Growth Des.*, 2017, **17**, 6262.
37 Q. Chen, P.-C. Guo, S.-P. Zhao, J.-L. Liu and X.-M. Ren, *CrystEngComm*, 2013, **15**, 1264.
38 B. A. Ramanan, *J. Mol. Struct.*, 2017, **1131**, 171.
39 M. Usman, C.-H. Lee, D.-S. Hung, S.-F. Lee, C.-C. Wang, T.-T. Luo, L. Zhao, M.-K. Wu and K.-L. Lu, *J. Mater. Chem. C*, 2014, **2**, 3762.
40 B. Garai, A. Mallick and R. Banerjee, *Chem. Sci.*, 2016, **7**, 2195.
41 M.-H. You, M.-H. Li, H.-H. Li, Y. Chen and M.-J. Lin, *Dalton Trans.*, 2019, **48**, 17381.
42 Z. Wang, L. Zeng, C. He and C. Duan, *ACS Appl. Mater. Interfaces*, 2022, **14**, 7980.
43 K. Liu, L. Wang, S. Li, H. Liu, D. Zhang, M. Jiang, W. Chen, F. Jiao, X. Zhang and W. Hu, *Adv. Funct. Mater.*, 2023, **33**, 2306871.
44 L. Zeng, T. Zhang, R. Liu, W. Tian, K. Wu, J. Zhu, Z. Wang, C. He, J. Feng, X. Guo, A. Ibro Douka and C. Duan, *Nat. Commun.*, 2023, **14**, 4002.
45 W.-B. Li, Y. Wu, X.-F. Zhong, X.-H. Chen, G. Liang, J.-W. Ye and Z.-W. Mo, *Angew. Chem., Int. Ed.*, 2023, **62**, e202303500.
46 X. Guo, N. Zhu, S.-P. Wang, G. Li, F.-Q. Bai, Y. Li, Y. Han, B. Zou, X.-B. Chen, Z. Shi and S. Feng, *Angew. Chem., Int. Ed.*, 2020, **59**, 19716.
47 X. Duan, J. Lin, Y. Li, C. Zhu and Q. Meng, *CrystEngComm*, 2008, **10**, 207.
48 G.-D. Lu, Z.-H. Zhang, Y.-Y. Tong, X.-M. Liu, X.-F. Ma and X.-P. Xuan, *Chem. – Asian J.*, 1970, **2019**, 14.
49 B. Zhao, S.-L. Li, Y.-N. Gu, Q.-Z. Sun and H. Liu, *J. Mol. Struct.*, 2022, **1270**, 133944.
50 Y.-Y. Jia, X.-T. Liu, W.-H. Wang, L.-Z. Zhang and X.-H. Bu, *Philos. Trans. R. Soc., A*, 2017, **375**, 20160026.
51 Q.-G. Zhai, X. Bu, C. Mao, X. Zhao and P. Feng, *J. Am. Chem. Soc.*, 2016, **138**, 2524.
52 W. Chen, Z. Wang, Q. Wang, K. El-Yanboui, K. Tan, H. M. Barkholtz, D.-J. Liu, P. Cai, L. Feng, Y. Li, J.-S. Qin, S. Yuan, D. Sun and H.-C. Zhou, *J. Am. Chem. Soc.*, 2023, **145**, 4736.

53 S. R. Miller, E. Alvarez, L. Fradcourt, T. Devic, S. Wutke, P. S. Wheatley, N. Steunou, C. Bonhomme, C. Gervais, D. Laurencin, R. E. Morris, A. Vimont, M. Daturi, P. Horcajada and C. Serre, *Chem. Commun.*, 2013, **49**, 7773.
54 Y. Wang, W. Fan, X. Wang, D. Liu, Z. Huang, F. Dai and J. Gao, *Polyhedron*, 2018, **155**, 261.
55 K. I. Hadjiivanov, D. A. Panayotov, M. Y. Mihaylov, E. Z. Ivanova, K. K. Chakarova, S. M. Andonova and N. L. Drenchev, *Chem. Rev.*, 2021, **121**, 1286.
56 M. Teixeira and S. A. Baudron, *CrystEngComm*, 2024, **26**, 5978.
57 L. Asgharnejad, A. Abbasi, M. Najafi and J. Janczak, *Cryst. Growth Des.*, 2019, **19**, 2679.
58 P.-K. Wang, W.-F. Wang, B.-Y. Li, M. J. Xie, H.-Y. Bian, S.-H. Wang, F.-K. Zheng and G.-C. Guo, *Inorg. Chem. Front.*, 2023, **10**, 5710.
59 J. Zhao, S. Ji, Y. Chen, H. Guo and P. Yang, *Phys. Chem. Chem. Phys.*, 2012, **14**, 8803.
60 J. D. Furman, A. Y. Warner, S. J. Teat, A. A. Mikhailovsky and A. K. Cheetam, *Chem. Mater.*, 2010, **22**, 2255.
61 L. Zhai, Z.-X. Yang, W.-W. Zhang, J.-L. Zuo and X.-M. Ren, *J. Mater. Chem. C*, 2018, **6**, 7030.
62 G. M. Sheldrick, *Acta Crystallogr., Sect. A:Found. Adv.*, 2015, **71**, 3.
63 G. M. Sheldrick, *Acta Crystallogr., Sect. C:Struct. Chem.*, 2015, **71**, 3.
64 *M86-EXX278V1 APEX4 User Manual*, Bruker Corporation, 2021.
65 *CrysAlisPro Software System, Version 1.171.43.70a*, Rigaku Oxford Diffraction, 2023.

